Digital In-Line Holography for the 3D-vizualization of inclusions in a droplet

Sébastien Coëtmellec, Darawan Pejchang, Wisuttida Wichitwong, Daniel Allano, Gérard Gréhan, Denis Lebrun, Marc Brunel*

UMR 6614 CORIA, Normandie Université, CNRS, Université et INSA de Rouen, Saint-Etienne du Rouvray, France
*corresponding author: marc.brunel@coria.fr

Abstract We have developed models that allow the description of digital in-line holography experiments with complex imaging systems, in terms of optical transfer matrices. The objects can be opaque, transparent or semi-transparent circular particles. In this presentation, we present the description of non-uniform objects whose transmission coefficient is decomposed on a basis of Zernike polynomials. Analytical expressions of the holograms are obtained. Digital holograms are reconstructed using the 2-dimensional fractional-order Fourier transform. The formalism is used to extract the 3D position of micrometric opaque and transparent inclusions in a suspended millimetric droplet. In a second step, a long-exposure time set-up is used. From the recorded holograms, the reconstruction of sections of the trajectories of a micronic particle within the droplet, using a sole hologram and a sole reconstruction, are shown. The exposure time is optimized in order to conserve a sufficient Signal to Noise ratio. In a last experiment, 50 nm SiO_2 nanoparticles are inserted in the droplet. A heating point is created in the droplet using a frequency-doubled Nd:YAG laser. A layer of vapor is then created around the nanometric inclusion. It grows into a cavitation air bubble of several micrometers whose position will be detected and reconstructed using our digital-holography set-up, and the formalism that we have developed. These developments should have important applications for the detection of nanoparticles, or for the visualization of freezing processes in a droplet.
Keywords: digital holography, droplets, inclusions, nanoparticles

1 Theoretical background on digital holography

The detection and characterization of particles inside droplets play an important role in many areas such as biology, climatology, public health microfluidics. In this study, the characterization of inclusions inside a water droplet is investigated by Digital In-line Holography (DIH) [1]. Digital holography has now applications in many domains from investigation of particles in flows [2-8], to visualization of cells in biology or medicine [9], to phase contrast metrology [10-12], or to detection of nanoparticles [13]. This technique will be shown to allow the measurement of size, 3D location and trajectory of inclusions in a droplet. Digital Holography is a non-invasive technique which consists of a laser, the object under interest and an electronic array sensor (as a CCD sensor). The in-line configuration allows the design of a simple set-up with a relatively low number of optical elements. The set-up that will be considered in this section is reported on figure 1. A Gaussian laser beam is emitted by a laser. It is sent toward different optical elements and focused in a suspended millimetric droplet. The in-line hologram is then recorded on a CCD sensor. From theoretical point of view, this set-up can be described using a scalar diffraction model [14-16]. The expression of the electric field in the plane of the sensor can be written:

$$E_{CCD}(x,y) = \frac{\exp\left(\frac{i2\pi\ell}{\lambda}\right)}{i\lambda\sqrt{B_2^x B_2^y}} \iint_{\mathbb{R}^2} E_p(\xi,\eta) T(\xi,\eta) \exp\left(\frac{i\pi\left(A_2^x\xi^2 - 2\xi x + D_2^x x^2\right)}{\lambda B_2^x}\right) \exp\left(\frac{i\pi\left(A_2^y\eta^2 - 2\eta y + D_2^y y^2\right)}{\lambda B_2^y}\right) d\xi d\eta \quad (1)$$

where λ is the wavelength of the laser beam. ℓ is the optical path between the particle and the CCD sensor. . $T(\xi,\eta)$ is the transmission coefficient of the particle. $E_p(\xi,\eta)$ is the expression of the incident gaussian beam in the plane of the CCD sensor. It is given using the classical formula of Gaussian beam propagation. Its expression could thus be written using the coefficients of the optical transfer matrix between the initial plane of the laser and the plane of the particle : A_1^x, B_1^x, D_1^x, A_1^y, B_1^y, D_1^y (for both transverse axes x and y). The coefficients A_2^x, B_2^x, D_2^x, A_2^y, B_2^y, D_2^y, are the coefficients of the optical transfer matrix from the plane of the particle to the plane of the CCD sensor.

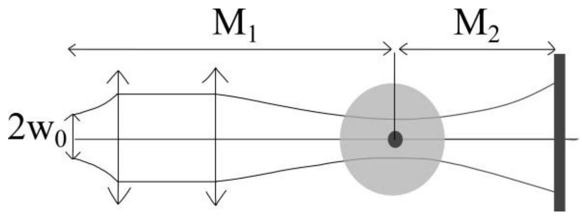

Fig. 1 Digital In-Line Holography set-up

The most complex part is to evaluate correctly the transmission coefficient $T(\xi,\eta)$ of the particle, and then the evaluation of integral (1). With this formalism, the droplet appears just as an optical element of the whole set-up. It is taken into account through the appropriate definition of the transfer matrices M_1^p and matrices M_2^p (with p = x or y). Note that the x and y matrices are identical when the elements of the system are spherical, and the droplet itself is spherical. The x and y matrices are different when the optical system contains cylindrical optical elements or an ellipsoidal droplet. We have developed theoretical studies where the transmission coefficient is expanded over a basis of Zernike polynomials. We can thus describe a wide range of particles (opaque, semi-transparent, transparent, aberrating particles). Analytical expression of $E_p(\xi,\eta)$ can then be obtained, which depend on the different parameters of the set-up [17,18].
The reconstruction is then performed using the 2 dimensional fractional Fourier transform (2D-FRFT) whose definition can be found in previous reference [14]. The numerical reconstruction can be viewed as a numerical refocusing on the diffracting element (particle inside the droplet in this study).
Experimentally, the laser used is a Continuous Wave, fibered-laser diode operating at 25°C, and emitting at wavelength 642nm (LP642-SF20, THORLABS).

2 Digital reconstruction of micronic inclusions in a millimetric droplet

a) Opaque inclusions in a bubble

Depending on the inclusion introduced into the droplet, different transmission coefficients $T(\xi,\eta)$ have to be considered. The most simple case is when the inclusion is a circular opaque particle. In this case, figure 2 (a) shows a simulated hologram of 20µm opaque particles dispersed in a millimetric water droplet. The hologram of Fig. 2(a) has then been numerically reconstructed by using an optimal 2D-FRFT. Fig. 2 (b) and is the optimal reconstruction where the different opaque particles appear.

.

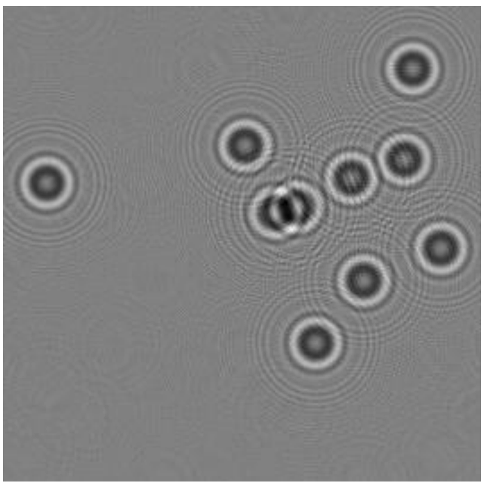

(a)

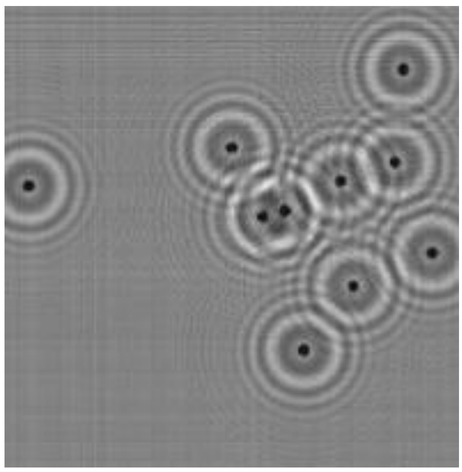

(b)

Fig. 2 Simulated hologram of 20µm particles (a) and optimal reconstruction (b)

b) Transparent microsphere in a bubble

If the inclusion is a transparent sphere, the transmission function has to be adapted to this new case. Figure 3(a) shows an experimental hologram while figure 3(b) shows the optimal reconstruction of the inclusion. In this case, the reconstructed object is characterized by a brilliant peak in the center of the opaque circle. This is confirmed by figure 4 that shows the x-axis and y-axis profiles of the reconstructed object.

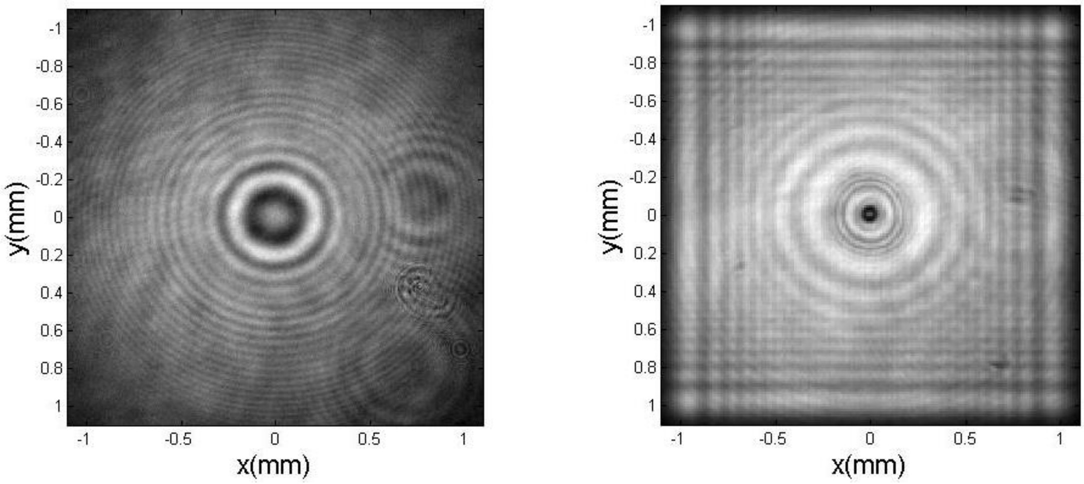

Fig. 3 Digital In-Line Hologram of a 20 μm glass microsphere located in a droplet and its optimal reconstruction

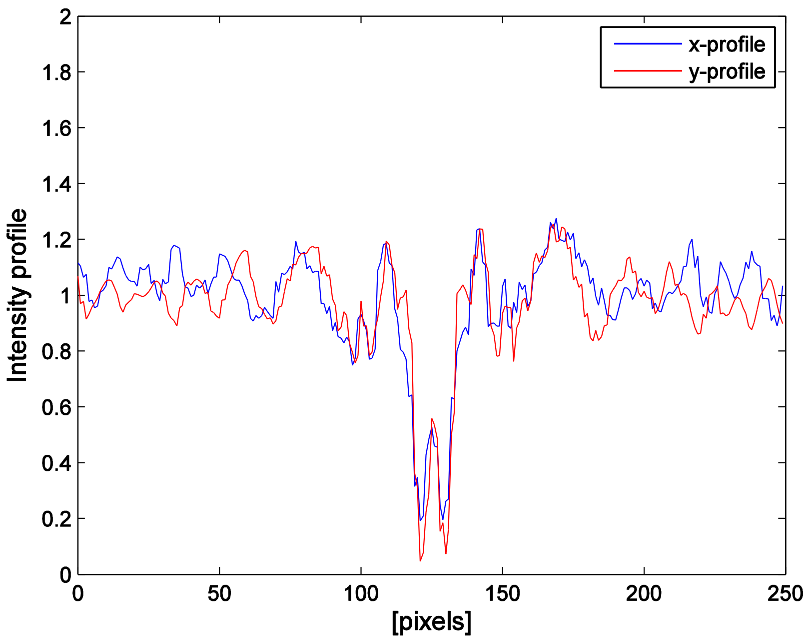

Fig. 4 x-axis and y-axis profiles of the reconstructed microsphere.

This case can be described theoretically by modelling the microsphere as a small lens introducing a quasi-spherical phase. Experiments are then well corroborated by the simulations [17].

c) Air microbubble in a droplet

If the inclusion is an air bubble, the transmission function has to be modified again. It is illustrated on the figure 5. As the index of air is smaller than the index of water, the bubble acts as a lens in its center, and as an opaque ring on its border (due to total reflection). The transmission function has then to be described by as a quasi-quadratic phase component (for the center of a bubble) combined to an opaque ring [18]. An exemple of experimental result will be given in section 4 when detecting nanoparticles.

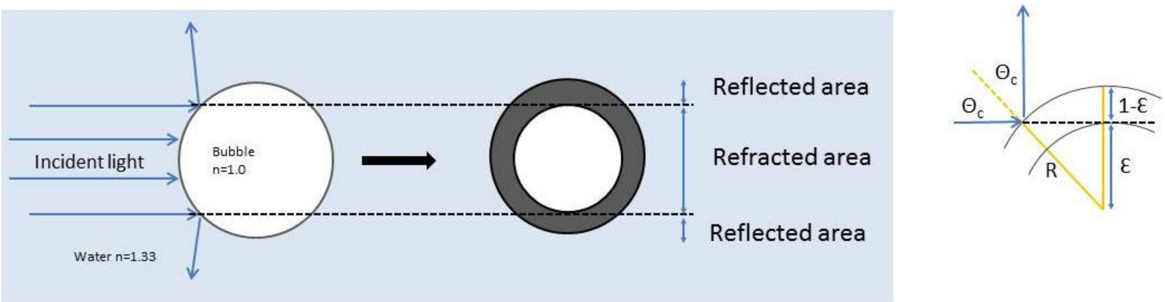

Fig. 5 Bubble in a liquid (reflected and refracted light)

3 Long exposure time experiments for visualization of the trajectory of inclusions

When the exposure time is much longer than the time necessary for grabbing the particle at one location, the diffraction pattern is spread along the trajectory of the particle [19,20]. Fig. 2(a) shows an experimental hologram recorded when the exposure time is 0.15s. After optimal reconstruction, we can further observe the trajectories of a given inclusion, which corresponds to the addition to the different axial positions of the inclusions. From the trajectory of the particles and the value of the exposure time, we can finally evaluate the transverse velocity of the inclusions. In this experiment, the moving particles inside the droplet are 20µm circular opaque particles. The laser is the CW- fibered laser-diode previously mentioned.
In this case, figure 6 (left) shows an experimental hologram recorded with the CCD sensor. The hologram has then been numerically reconstructed by using an optimal 2D-FRFT for one particle (in the red circle). The trajectory of the particles and its transverse velocity can be evaluated from this reconstruction. At this stage, the accuracy in numerical reconstruction process is not sufficient to evaluate the longitudinal velocity of the particle. The exposure time has to be optimized in order to conserve a sufficient Signal to Noise ratio [20].

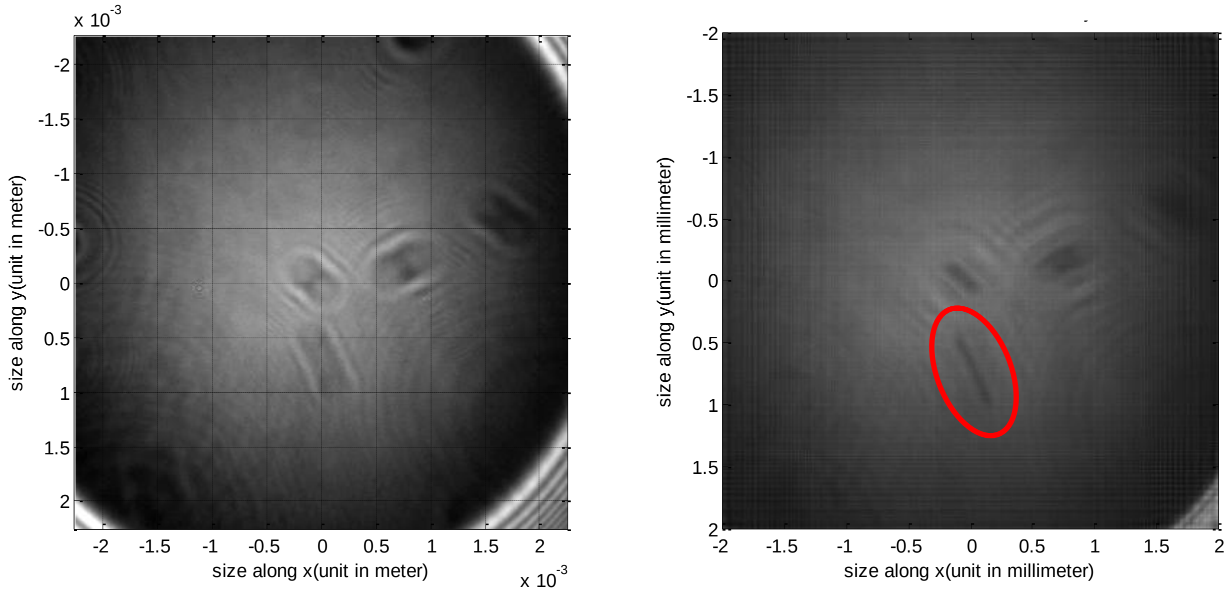

Fig. 6 Experimental hologram of 20 µm inclusions in a millimetric droplet using a long exposure time (left) and optimal reconstruction of one of the particles (right).

4 Detection of nanoparticles in a millimetric droplet

We consider now the set-up of figure 7. A laser beam (emitted by a fibered-laser diode) is collimated and then focused in the vicinity of a suspended water droplet using a microscope objective. The wavelength of this beam is 642 nm. The light is then collected with a second microscope objective and a CCD sensor is positioned in order to record digital in-line holograms. The diameter of the water droplet is 1.5 mm (with refractive index 1.33). Nanoparticles (with a calibrated diameter of 50 nm) are introduced into the droplet. The droplet is then heated using a frequency-doubled, pulsed Nd:YAG laser (pulse duration 5ns). Heating a nanoparticle creates a surrounding microbubble. The hologram of this bubble is recorded on the CCD sensor. The microbubble is finally reconstructed using a 2D-FRFT operation. Figure 8 shows a typical experimental hologram recorded with this set-up. The hologram created by a microbubble is observed in the red frame. This hologram is then optimally reconstructed using 2D-FRFT. The experimental reconstruction is presented in figure 9 (left). It is characterized by an opaque disk with an intense peak in its center, in good accordance with theoretical predictions (right) that could be done modelling the microbubble as described in section 2.c. A radial profile of the reconstructed micro-droplet is presented in figure 10. From the value of its width and the value of the magnification factor introduced by the microscope objective Obj2and the output surface of the droplet itself, the size of the microbubble can be deduced. This indirect detection method is particularly efficient. Note that it is possible to estimate the size of the nanoparticles from the size of the microbubble and the characteristics of the laser beam [21,22].

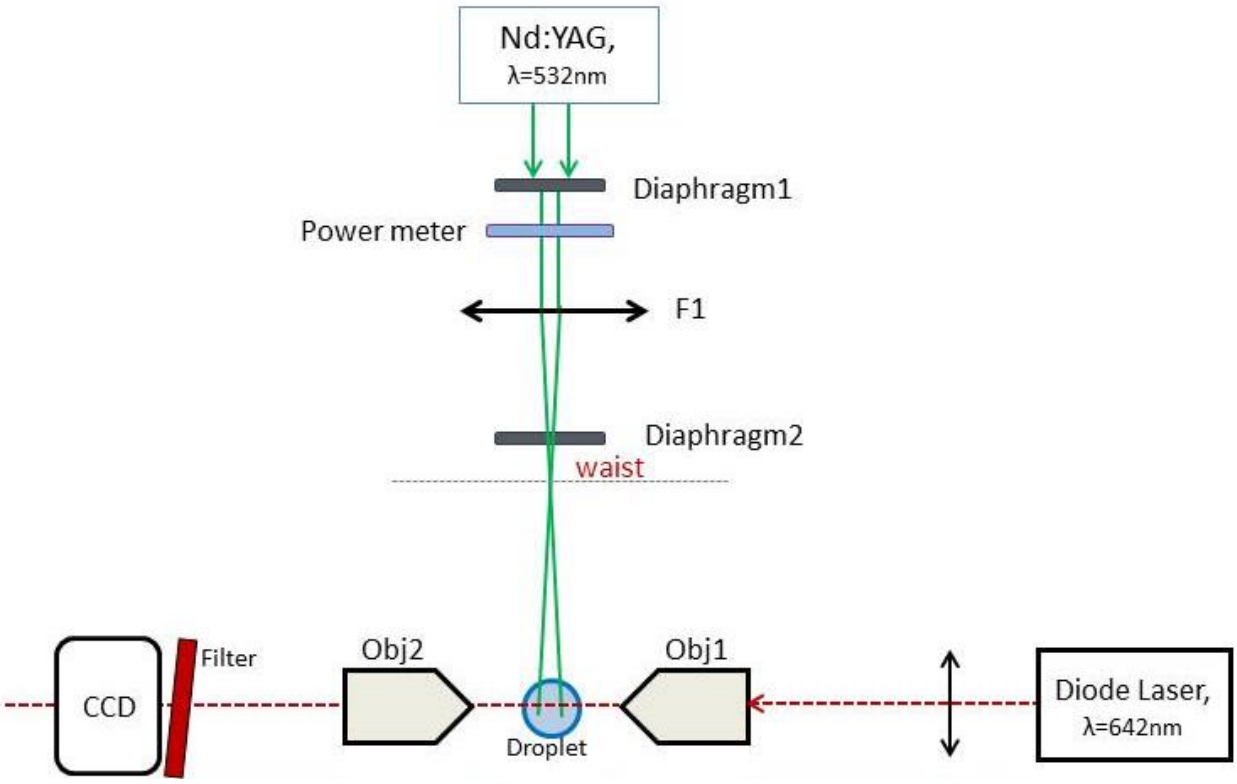

Fig. 7 Experimental digital in-line holography set-up to detect nanoparticles in a droplet

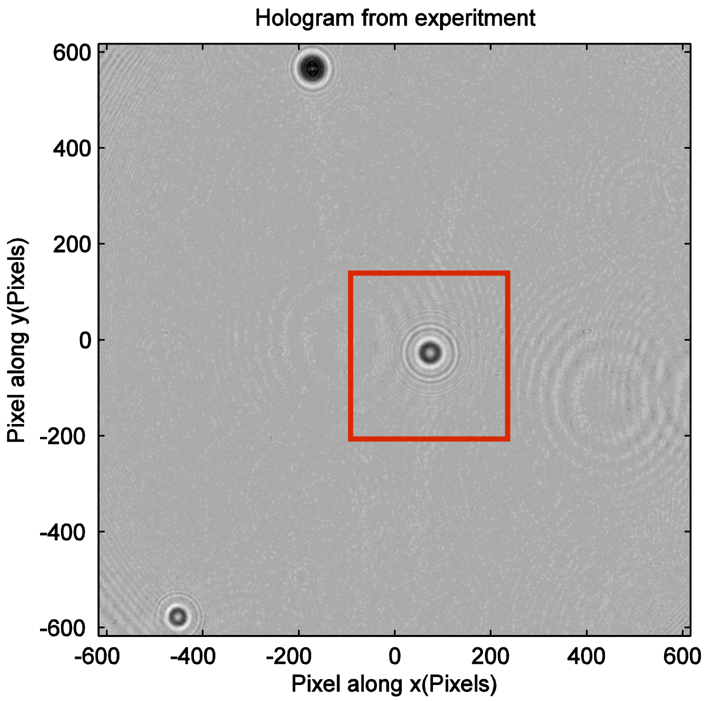

Fig. 8 Typical experimental hologram obtained after heating of a nanoparticle in the droplet

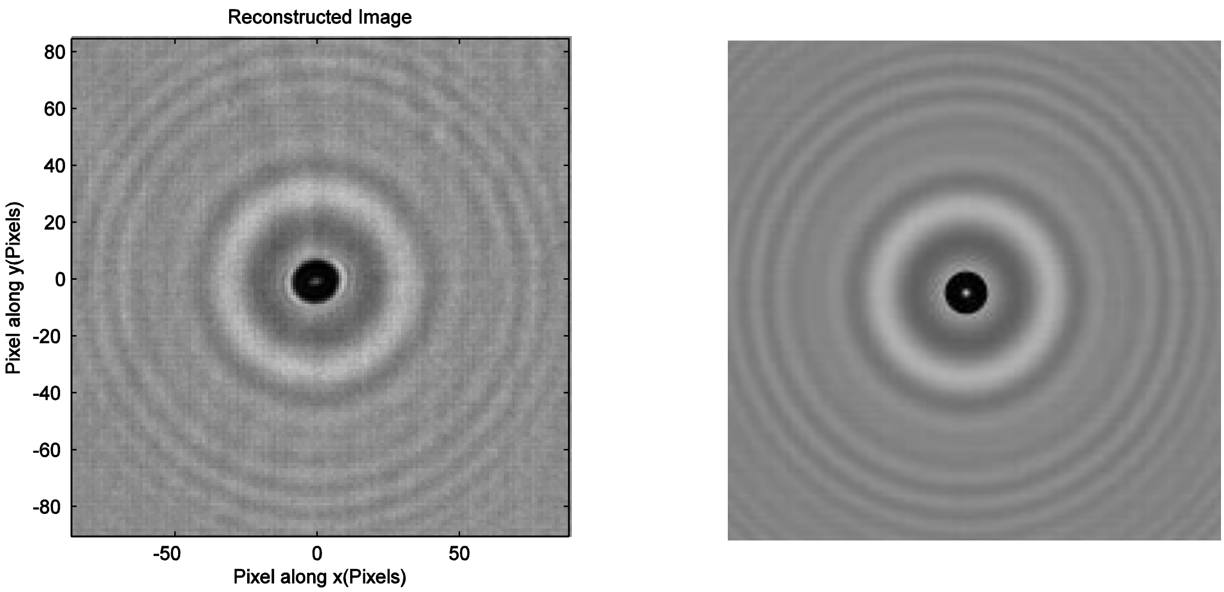

Fig. 9 Optimal reconstruction of the micro-bubble: experimental (left) and corresponding simulation (right)

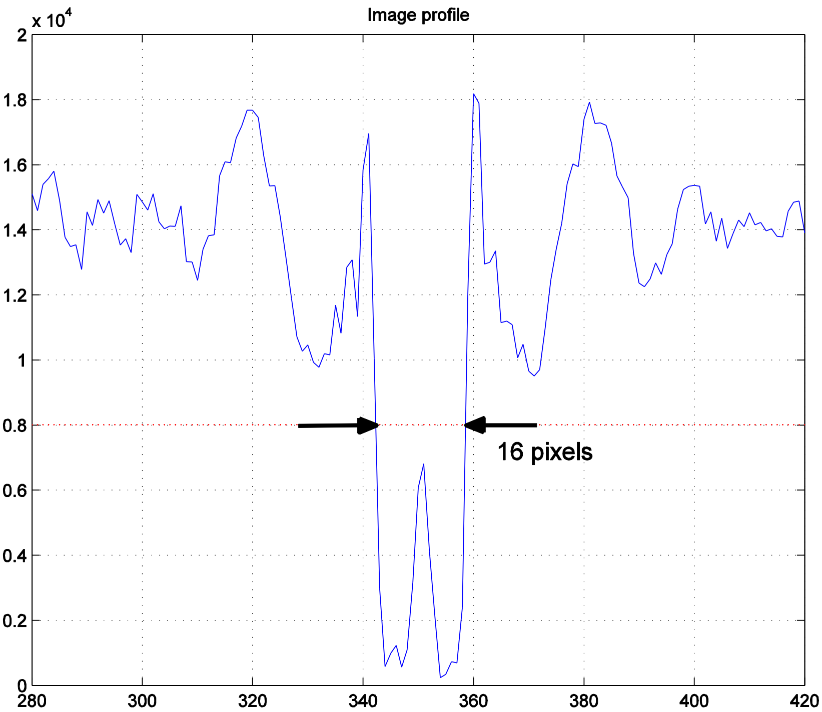

Fig. 10 Radial profile of the reconstructed micro-bubble

5 Conclusion

We have developed models that allow the description of digital in-line holography experiments with complex imaging systems. The scattering elements under study can be either opaque, transparent or semi-transparent particles. Digital holograms are reconstructed using the 2-dimensional fractional-order Fourier transform. The formalism is used to reconstruct micrometric inclusions in a suspended millimetric droplet. Their 3D position in the droplet can be extracted. Long-exposure time experiments allow the reconstruction of sections of the trajectories of these micronic particle within the droplet using a sole hologram. Finally, 50 nm SiO_2 nanoparticles are inserted in the droplet. A heating point is created in the droplet using a frequency-doubled Nd:YAG laser, creating a layer of vapor around the nanometric inclusion. A cavitation air bubble of several micrometers can then be reconstructed using digital holography, which allows an indirect detection of the nanoparticles. These developments should have important applications for the detection of nanoparticles.

Acknowledgments

The authors thank the French National Agency under grant ANR-2011-NANO-008 NANOMORPH for financial support and through the program Investissements d'Avenir (ANR-10-LABX-09-01) LabEx EMC[3].

References

[1] Schnars U, Jüptner W P (1994) Direct recording of holograms by a CCD target and numerical reconstruction, *Applied Optics*, vol. 33, pp 179-181. doi: http://dx.doi.org/10.1364/AO.33.000179

[2] Katz J, Sheng J (2010) Applications of Holography in Fluid Mechanics and Particle Dynamics, *Annual Review of Fluid Mechanics,* vol. 42, pp 531-555. doi: 10.1146/annurev-fluid-121108-145508

[3] Buraga-Lefebvre C, Coetmellec S, Lebrun D, Ozkul C (2000) Application of wavelet transform to hologram analysis: three-dimensional location of particles, *Optics and Lasers in Engineering*, vol. 33, pp 409-421. doi:10.1016/S0143-8166(00)00050-6

[4] Xu W, Jericho M H, Kreuzer H J, Meinertzhagen I A (2003) Tracking particles in four dimensions with in-line holographic microscopy, *Optics Letters,* vol. 28, pp 164-166. doi:

http://dx.doi.org/10.1364/OL.28.000164

[5] Pan G, Meng H (2003) Digital holography of particle fields: reconstruction by use of complex amplitude, Applied Optics, vol. 42, pp 827-833. doi: http://dx.doi.org/10.1364/AO.42.000827

[6] Denis L, Fournier C, Fournel T, Ducottet C, Jeulin D (2006) Direct extraction of the mean particle size from a digital hologram, Applied Optics, vol. 45, pp 944-952. doi: http://dx.doi.org/10.1364 /AO.45.000944

[7] Desse J M, Picart P, Tankam P (2008) Digital three-color holographic interferometry for flow analysis, *Optics Express*, vol. 16, pp 5471-5480. doi: http://dx.doi.org/10.1364/OE.16.005471

[8] Verrier N, Remacha C, Brunel M, Lebrun D, Coëtmellec S (2010) Micropipe flow visualization using digital in-line holographic microscopy, *Optics Express*, vol. 18, pp 7807-7819. doi: http://dx.doi.org/10.1364/OE.18.007807

[9] Kim M K, (2000) Tomographic three-dimensional imaging of a biological specimen using wavelength-scanning digital interference holography, *Optics Express*, vol. 7, pp 305-310. doi: http://dx.doi.org/10.1364/OE.7.000305

[10] Cuche E, Marquet P, Depeursinge C (1999) Simultaneous amplitude-contrast and quantitative phase-contrast microscopy by numerical reconstruction of Fresnel off-axis holograms, *Applied Optics*, vol. 38, pp 6994-7001. doi: http://dx.doi.org/10.1364/AO.38.006994

[11] Brunel M, Coëtmellec S, Lebrun D, Ait Ameur K (2009) Digital phase contrast with the fractional Fourier transform, *Applied Optics*, vol. 48, pp 579-583. doi: http://dx.doi.org/10.1364/AO.48.000579

[12] Brunel M, Shen H, Coëtmellec S, Lebrun D, Ait Ameur K (2012) Femtosecond digital in-line holography with the fractional Fourier transform: application to phase-contrast metrology, *Applied Physics B*, vol. 106, pp 583-591. doi: 10.1007/s00340-011-4782-y

[13] Absil E, Tessier G, Gross M, Atlan M, Warnasooriya N, Suck S, Coppey-Moisan M, Fournier D (2010) Photothermal heterodyne holography of gold nanoparticles, *Optics Express*, vol. 18, pp 780-786. doi: http://dx.doi.org/10.1364/OE.18.000780

[14] Verrier N, Coëtmellec S, Brunel M, Lebrun D (2008) Digital in-line holography in thick optical systems: application to visualization in pipes, *Applied Optics*, vol. 47, pp 4147-4157. doi: http://dx.doi.org/10.1364/AO.47.004147

[15] Brunel M, Shen H, Coëtmellec S, Lebrun D, Aït Ameur K (2013) Phase contrast metrology using digital in-line holography: general models and reconstruction of phase discontinuities. *Journal of Quantitative Spectroscopy and Radiative Transfer*, vol. 126, pp 113-121. doi: http://dx.doi.org/10.1016/j.jqsrt. 2012.08.015

[16] Brunel M, Wichitwong W, Coëtmellec S, Masselot A, Lebrun D, Gréhan G, Edouard G (2015) Numerical models for exact description of in-situ Digital In-Line Holography experiments with irregularly-shaped arbitrarily-located particles, to appear in *Applied Sciences*.

[17] Coëtmellec S, Wichitwong W, Gréhan G, Lebrun D, Brunel M, Janssen A J E M (2014) Digital in-line holography assessment for general phase and opaque particle. *Journal of the European Optical Society: Rapid Publications*, vol. 9, 14021. doi: http://dx.doi.org/10.2971/jeos.2014.14021

[18] Coëtmellec S, Pejchang D, Allano D, Gréhan G, Lebrun D, Brunel M, Janssen A J E M (2014) Digital in-line holography in a droplet with cavitation air bubbles, *Journal of the European. Optical Society: Rapid Publications*, vol. 9, 14056. doi: http://dx.doi.org/10.2971/jeos.2014.14056

[19] Lebrun D, Méès L, Fréchou D, Coëtmellec S, Brunel M, Allano D (2013) Long time exposure digital in-line holography for 3-D particle trajectography, *Optics Express*, vol. 21, pp 23522-23530. doi: http://dx.doi.org/10.1364/OE.21.023522

[20] Wichitwong W, Coëtmellec S, Lebrun D, Allano D, Gréhan G, Brunel M (2014) Long exposure time Digital In-line Holography for the trajectography of micronic particles within a suspended millimetric droplet. *Optics Communications*, vol. 326, pp 160-165. http://dx.doi.org/10.1016/j.optcom.2014.04.013

[21] Chaari A, Grosges T, Giraud-Moreau L, Barchiesi D (2013) Nanobubble evolution around nanowire in liquid, *Optics Express*, vol. 21, pp 26942–26954. http://dx.doi.org/10.1364/OE.21.026942

[22] Chaari A, Grosges T, Giraud-Moreau L, Barchiesi D (2014) Numerical Modeling of the Photothermal Processing for Bubble Forming around Nanowire in a Liquid, *The Scientific World Journal*, vol. 2014, pp 794630. doi: http://dx.doi.org/10.1155/2014/794630